

Observation of Exclusive $\bar{B} \rightarrow D^{(*)}K^{*-}$ Decays

CLEO Collaboration

(December 11, 2001)

Abstract

We report the first observation of the exclusive decays $\bar{B} \rightarrow D^{(*)}K^{*-}$, using 9.66×10^6 $B\bar{B}$ pairs collected at the $\Upsilon(4S)$ with the CLEO detector. We measure the following branching fractions: $\mathcal{B}(B^- \rightarrow D^0 K^{*-}) = (6.1 \pm 1.6 \pm 1.7) \times 10^{-4}$, $\mathcal{B}(\bar{B}^0 \rightarrow D^+ K^{*-}) = (3.7 \pm 1.5 \pm 1.0) \times 10^{-4}$, $\mathcal{B}(\bar{B}^0 \rightarrow D^{*+} K^{*-}) = (3.8 \pm 1.3 \pm 0.8) \times 10^{-4}$ and $\mathcal{B}(B^- \rightarrow D^{*0} K^{*-}) = (7.7 \pm 2.2 \pm 2.6) \times 10^{-4}$. The $\bar{B} \rightarrow D^* K^{*-}$ branching ratios are the averages of those corresponding to the 00 and 11 helicity states. The errors shown are statistical and systematic, respectively.

R. Mahapatra,¹ H. N. Nelson,¹ R. A. Briere,² G. P. Chen,² T. Ferguson,² G. Tatishvili,²
H. Vogel,² N. E. Adam,³ J. P. Alexander,³ C. Bebek,³ K. Berkelman,³ F. Blanc,³
V. Boisvert,³ D. G. Cassel,³ P. S. Drell,³ J. E. Duboscq,³ K. M. Ecklund,³ R. Ehrlich,³
L. Gibbons,³ B. Gittelman,³ S. W. Gray,³ D. L. Hartill,³ B. K. Heltsley,³ L. Hsu,³
C. D. Jones,³ J. Kandaswamy,³ D. L. Kreinick,³ A. Magerkurth,³ H. Mahlke-Krüger,³
T. O. Meyer,³ N. B. Mistry,³ E. Nordberg,³ M. Palmer,³ J. R. Patterson,³ D. Peterson,³
J. Pivarski,³ D. Riley,³ A. J. Sadoff,³ H. Schwarthoff,³ M. R. Shepherd,³ J. G. Thayer,³
D. Urner,³ B. Valant-Spaight,³ G. Viehhauser,³ A. Warburton,³ M. Weinberger,³
S. B. Athar,⁴ P. Avery,⁴ H. Stoeck,⁴ J. Yelton,⁴ G. Brandenburg,⁵ A. Ershov,⁵
D. Y.-J. Kim,⁵ R. Wilson,⁵ K. Benslama,⁶ B. I. Eisenstein,⁶ J. Ernst,⁶ G. D. Gollin,⁶
R. M. Hans,⁶ I. Karliner,⁶ N. Lowrey,⁶ M. A. Marsh,⁶ C. Plager,⁶ C. Sedlack,⁶ M. Selen,⁶
J. J. Thaler,⁶ J. Williams,⁶ K. W. Edwards,⁷ R. Ammar,⁸ D. Besson,⁸ X. Zhao,⁸
S. Anderson,⁹ V. V. Frolov,⁹ Y. Kubota,⁹ S. J. Lee,⁹ S. Z. Li,⁹ R. Poling,⁹ A. Smith,⁹
C. J. Stepaniak,⁹ J. Urheim,⁹ S. Ahmed,¹⁰ M. S. Alam,¹⁰ L. Jian,¹⁰ M. Saleem,¹⁰
F. Wappler,¹⁰ E. Eckhart,¹¹ K. K. Gan,¹¹ C. Gwon,¹¹ T. Hart,¹¹ K. Honscheid,¹¹
D. Hufnagel,¹¹ H. Kagan,¹¹ R. Kass,¹¹ T. K. Pedlar,¹¹ J. B. Thayer,¹¹ E. von Toerne,¹¹
T. Wilksen,¹¹ M. M. Zoeller,¹¹ H. Muramatsu,¹² S. J. Richichi,¹² H. Severini,¹² P. Skubic,¹²
S.A. Dytman,¹³ S. Nam,¹³ V. Savinov,¹³ S. Chen,¹⁴ J. W. Hinson,¹⁴ J. Lee,¹⁴ D. H. Miller,¹⁴
V. Pavlunin,¹⁴ E. I. Shibata,¹⁴ I. P. J. Shipsey,¹⁴ D. Cronin-Hennessy,¹⁵ A.L. Lyon,¹⁵
C. S. Park,¹⁵ W. Park,¹⁵ E. H. Thorndike,¹⁵ T. E. Coan,¹⁶ Y. S. Gao,¹⁶ F. Liu,¹⁶
Y. Maravin,¹⁶ I. Narsky,¹⁶ R. Stroynowski,¹⁶ J. Ye,¹⁶ M. Artuso,¹⁷ C. Boulahouache,¹⁷
K. Bukin,¹⁷ E. Dambasuren,¹⁷ G. C. Moneti,¹⁷ R. Mountain,¹⁷ T. Skwarnicki,¹⁷ S. Stone,¹⁷
J.C. Wang,¹⁷ A. H. Mahmood,¹⁸ S. E. Csorna,¹⁹ I. Danko,¹⁹ Z. Xu,¹⁹ G. Bonvicini,²⁰
D. Cinabro,²⁰ M. Dubrovin,²⁰ S. McGee,²⁰ A. Bornheim,²¹ E. Lipeles,²¹ S. P. Pappas,²¹
A. Shapiro,²¹ W. M. Sun,²¹ A. J. Weinstein,²¹ G. Masek,²² and H. P. Paar²²

¹University of California, Santa Barbara, California 93106

²Carnegie Mellon University, Pittsburgh, Pennsylvania 15213

³Cornell University, Ithaca, New York 14853

⁴University of Florida, Gainesville, Florida 32611

⁵Harvard University, Cambridge, Massachusetts 02138

⁶University of Illinois, Urbana-Champaign, Illinois 61801

⁷Carleton University, Ottawa, Ontario, Canada K1S 5B6

and the Institute of Particle Physics, Canada M5S 1A7

⁸University of Kansas, Lawrence, Kansas 66045

⁹University of Minnesota, Minneapolis, Minnesota 55455

¹⁰State University of New York at Albany, Albany, New York 12222

¹¹Ohio State University, Columbus, Ohio 43210

¹²University of Oklahoma, Norman, Oklahoma 73019

¹³University of Pittsburgh, Pittsburgh, Pennsylvania 15260

¹⁴Purdue University, West Lafayette, Indiana 47907

¹⁵University of Rochester, Rochester, New York 14627

¹⁶Southern Methodist University, Dallas, Texas 75275

¹⁷Syracuse University, Syracuse, New York 13244

¹⁸University of Texas - Pan American, Edinburg, Texas 78539

¹⁹Vanderbilt University, Nashville, Tennessee 37235

²⁰Wayne State University, Detroit, Michigan 48202

²¹California Institute of Technology, Pasadena, California 91125

²²University of California, San Diego, La Jolla, California 92093

The study of CP violation in B mesons provides a decisive test of the CP violation mechanism in the Standard Model (SM). In the SM, CP violation is the consequence of the complex phase in the Cabibbo-Kabayashi-Maskawa (CKM) quark-mixing matrix [1]. Comprehensive tests of the SM predictions on CP violation require precision measurements of the three sides and three angles of the CKM unitary triangle [2]. The angle γ can be measured using $\bar{B} \rightarrow D^{(*)}K^{(*)}$ decays [2,3]. The decay $B^- \rightarrow D^0 K^-$ was first observed at CLEO [4] and confirmed by BELLE [5]. In this Letter, we report the first observation of the exclusive hadronic B decays $\bar{B} \rightarrow D^{(*)}K^{*-}$. Charge-conjugate modes are implied throughout this Letter.

The data were collected with two configurations (CLEO II [6] and CLEO II.V [7]) of the CLEO detector at the Cornell Electron Storage Ring (CESR). The data consist of 9.13 fb^{-1} taken at the $\Upsilon(4S)$, which corresponds to 9.66×10^6 $B\bar{B}$ pairs, and 4.35 fb^{-1} taken below $B\bar{B}$ threshold, which is used for continuum background studies. We assume that the produced B^+B^- rate is the same as $B^0\bar{B}^0$ [8] at the $\Upsilon(4S)$.

Signal B meson candidates are fully reconstructed by combining detected photons and charged pions and kaons. The detector elements most important for the results presented here are the tracking system, which consists of several concentric detectors operating inside a 1.5 T superconducting solenoid, and the electromagnetic calorimeter, consisting of 7800 CsI(Tl) crystals. For CLEO II, the tracking system consisted of a 6-layer straw tube chamber, a 10-layer precision drift chamber, and a 51-layer main drift chamber. The main drift chamber also provided a measurement of the specific ionization loss, dE/dx , used for particle identification. For CLEO II.V, the straw tube chamber was replaced by a 3-layer, double-sided silicon vertex detector, and the gas in the main drift chamber was changed from an argon-ethane to a helium-propane mixture.

The particles in the final state are identified via the decay modes $K^{*-} \rightarrow K_S^0 \pi^-$ with $K_S^0 \rightarrow \pi^+ \pi^-$; $D^0 \rightarrow K^- \pi^+$, $K^- \pi^+ \pi^0$ and $K^- \pi^+ \pi^+ \pi^-$; $D^+ \rightarrow K^- \pi^+ \pi^+$; $D^{*+} \rightarrow D^0 \pi_s^+$; $D^{*0} \rightarrow D^0 \pi^0$ and $D^0 \gamma$. Reconstructed tracks are required to pass quality cuts based on the track fit residuals, the impact parameter in both the r - ϕ and r - z planes and the number of drift chamber measurements. The dE/dx measured by the main drift chamber is used to distinguish kaons from pions. Electrons are selected based on dE/dx information and the ratio of the associated shower energy in the calorimeter to the measured track momentum. Muons are selected by requiring that charged tracks penetrate more than five interaction lengths of material. Any hadron candidate is required not to be identified as an electron or a muon. Pairs of charged tracks used to reconstruct the K_S^0 's (via $K_S^0 \rightarrow \pi^+ \pi^-$) are required to have a common vertex displaced from the primary interaction point. The invariant mass of the two charged pions is required to be within 3 standard deviations ($\sigma \approx 3 \text{ MeV}$) of the nominal K_S^0 mass [9]. Furthermore, the K_S^0 momentum vector, obtained from a kinematic fit of the charged pions' momenta, is required to point back to the beam spot. To form π^0 candidates, pairs of photon candidates with an invariant mass within $[-3.0, 2.5]\sigma$ ($\sigma \approx 6 \text{ MeV}$) of the nominal π^0 mass are kinematically fitted with the mass constrained to the nominal π^0 mass [9]. The soft photon from $D^{*0} \rightarrow D^0 \gamma$ decay is required to have an energy of 100 MeV or greater, and a π^0 veto within $[-4.5, 3.5]\sigma$ of the π^0 mass is applied.

B meson candidates are identified through their measured mass and energy. There are two key variables for full reconstruction of B mesons at CLEO, which take advantage of the fact that the B meson energy is the same as the beam energy. One is the beam-constrained

mass of the candidate which is defined as $M_B \equiv \sqrt{E_{\text{beam}}^2 - |\mathbf{p}|^2}$, where \mathbf{p} is the measured momentum of the candidate and E_{beam} is the beam energy. The second observable, ΔE , is defined to be the sum of the energies of the decay products of the B candidate minus the beam energy, *i.e.*, $\Delta E \equiv E_B - E_{\text{beam}}$. $|\Delta E|$ will be large if a decay product of the B candidate has been lost or assigned the wrong particle species. For fully-reconstructed B meson decays, the M_B distribution peaks at 5.28 GeV with resolution around 3 MeV, and ΔE peaks at 0 GeV, with a resolution of about 15 MeV.

The K^{*-} is required to have a mass within 75 MeV of its nominal mass [9] and $D^0 \rightarrow K^-\pi^+$, $K^-\pi^+\pi^0$, $K^-\pi^+\pi^+\pi^-$ candidates are required to have masses within 16 MeV, 25 MeV and 14 MeV (2σ) of their nominal masses respectively [9]. For $D^0 \rightarrow K^-\pi^+\pi^0$, we further impose a Dalitz weight cut [10] which reduces the background by about 70% with only about a 20% efficiency loss. The mass differences between $D^{*+}(D^{*0})$ and D^0 are required to be within 2.0σ of their nominal values [9] ($\sigma \approx 0.8$ MeV for $D^{*+} \rightarrow D^0\pi_s^+$, 1.0 MeV for $D^{*0} \rightarrow D^0\pi^0$ and 4.0 MeV for $D^{*0} \rightarrow D^0\gamma$). Because the K^{*-} from $\bar{B} \rightarrow DK^{*-}$ decays is polarized, we further require $|\cos\alpha| > 0.4$, where α is the helicity angle between one of the K^{*-} decay products in the K^{*-} rest frame and the direction of the K^{*-} momentum in the B rest frame.

The main background comes from continuum $e^+e^- \rightarrow q\bar{q}$ events, where $q = u, d, s, c$. To suppress this background, we require that the ratio R_2 of the second to the zeroth Fox-Wolfman moments, determined using charged tracks and unmatched neutral showers, be less than 0.5. To further reduce continuum background, we require that the cosine of the angle between the sphericity axis [11] of the candidate tracks and the sphericity axis of the rest of the event be less than 0.9. The distribution of this angle should be flat for B mesons and strongly peaked near ± 1.0 for the continuum background.

Each K^{*-} candidate is combined with any $D^{(*)}$ candidate in the event to form a $\bar{B} \rightarrow D^{(*)}K^{*-}$ candidate. All the $\bar{B} \rightarrow D^{(*)}K^{*-}$ candidates are required to have ΔE within 2.5σ of zero, with the resolution varying from 12 to 20 MeV depending on the decay mode. In case of an event with multiple candidates, we select the one with the smallest $|\Delta E|$. Studies show that no significant bias is introduced by this procedure.

We combine all the sub-modes for each $\bar{B} \rightarrow D^{(*)}K^{*-}$ decay and fit the beam-constrained mass distributions using a binned maximum likelihood method with the mass resolution fixed at the value determined from Monte Carlo simulation. Studies of similar $\bar{B} \rightarrow D^{(*)}\pi^-$ modes show that the mass resolutions in the Monte Carlo samples and in the data are in good agreement. The beam-constrained mass distribution is modeled by a Gaussian plus the phenomenological background function [12]. The results for the $\bar{B} \rightarrow D^{(*)}K^{*-}$ modes are shown in Fig. 1 and summarized in Table I. Significant excesses of events are observed in the signal regions, compatible with our M_B and ΔE resolutions. These excesses are consistent with coming from $\bar{B} \rightarrow D^{(*)}K^{*-}$ decays.

To estimate the detection efficiencies, we generated $\bar{B} \rightarrow D^{(*)}K^{*-}$ Monte Carlo events and simulated the CLEO detector response with GEANT [13]. Simulated events for the CLEO II and II.V configurations were processed in the same manner as the data. The resulting detection efficiencies, which are listed in Table I, do not include the $D^{(*)}$ or K^{*-} decay branching fractions [9]. For the $\bar{B} \rightarrow D^{(*)}K^{*-}$ decays, as we do not know the polarization of the two vector mesons, we generated both 00 and 11 helicity states for our Monte Carlo signal events to calculate the efficiencies as shown in Tables I.

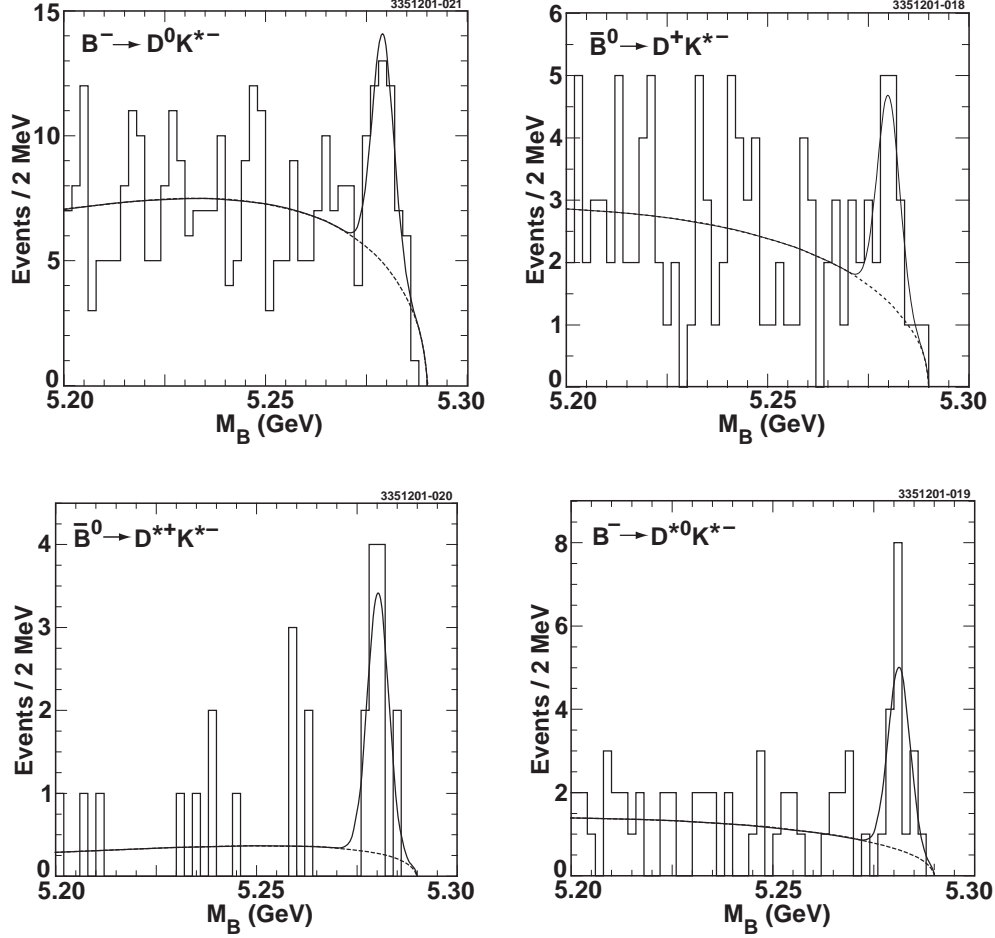


FIG. 1. The beam-constrained invariant mass distributions for $\bar{B} \rightarrow D^{(*)}K^{*-}$ decays with all sub-modes combined. The histograms show the data, the solid lines represent the overall fit to the data, and the dashed lines represent the fitted backgrounds under the peaks.

We use wrong-sign ($D^{(*)}K^{*+}$) combinations from the on-resonance sample and right-sign combinations from the continuum sample as cross-checks. For the wrong sign analysis, instead of searching for $D^{(*)}K^{*-}$ combinations where $K^{*-} \rightarrow K_S^0\pi^-$, we search for $D^{(*)}K^{*+}$ combinations where $K^{*+} \rightarrow K_S^0\pi^+$. The same selection cuts are applied for the wrong-sign candidates as for the right-sign ones. No enhancement is observed in the signal region for these wrong-sign combinations. We also apply the same selection criteria to the right-sign combinations in the continuum sample, and no enhancement is observed in the signal region.

Systematic errors from event selection include uncertainties in dE/dx , the Dalitz weight cut for $D^0 \rightarrow K^-\pi^+\pi^0$ and Monte Carlo statistics. To estimate the effects of the π^0 veto and the $E_\gamma > 100$ MeV requirement for the photon candidates in $D^{*0} \rightarrow D^0\gamma$ decays, we change the π^0 veto interval by 1σ and the energy cut value by ± 10 MeV respectively, and take the difference in the efficiency-corrected yields as the systematic error. The cross-feed rates between $\bar{B} \rightarrow D^{*0}K^{*-}$, where $D^{*0} \rightarrow D^0\pi^0$ and $D^{*0} \rightarrow D^0\gamma$, are less than 1.5%. We also use tighter and looser requirements of: $1\sigma/3\sigma$ for the $D^{(*)}$ mass cut, 50 MeV/100 MeV for the K^{*-} mass requirement, and 0.8/0.9 for the cosine of the sphericity angle to obtain

TABLE I. Results for the $\bar{B} \rightarrow D^{(*)}K^{*-}$ decay modes with statistical errors only. For $\bar{B} \rightarrow D^*K^{*-}$, the two efficiencies correspond to the 00 and 11 helicity states, respectively. The statistical significance of the overall signal for each mode is given in parentheses.

Decay Mode	Efficiency(%)	Yield	$\mathcal{B}(\times 10^{-4})$
$B^- \rightarrow D^0(K^-\pi^+)K^{*-}$	18.7	9.8 ± 3.7	6.2 ± 2.3
$B^- \rightarrow D^0(K^-\pi^+\pi^0)K^{*-}$	5.4	7.9 ± 4.4	4.9 ± 2.7
$B^- \rightarrow D^0(K^-\pi^+\pi^+\pi^-)K^{*-}$	10.7	11.9 ± 5.6	6.7 ± 3.2
$B^- \rightarrow D^0K^{*-}$		$30.5 \pm 8.3 (6.0\sigma)$	6.1 ± 1.6
$B^0 \rightarrow D^+(K^-\pi^+\pi^+)K^{*-}$	15.5	$11.5 \pm 4.7 (4.2\sigma)$	3.7 ± 1.5
$B^0 \rightarrow D^{*+}(D^0(K^-\pi^+)\pi_s^+)K^{*-}$	14.9, 17.1	0.8 ± 1.1	0.9 ± 1.3 0.8 ± 1.1
$\bar{B}^0 \rightarrow D^{*+}(D^0(K^-\pi^+\pi^0)\pi_s^+)K^{*-}$	4.7, 5.5	4.3 ± 2.3	4.5 ± 2.4 3.8 ± 2.0
$\bar{B}^0 \rightarrow D^{*+}(D^0(K^-\pi^+\pi^+\pi^-)\pi_s^+)K^{*-}$	6.5, 8.1	5.5 ± 2.5	7.5 ± 3.4 6.1 ± 2.8
$B^0 \rightarrow D^{*+}K^{*-}$		$10.5 \pm 3.5 (5.4\sigma)$	4.1 ± 1.4 3.5 ± 1.2
$B^- \rightarrow D^{*0}(D^0(K^-\pi^+)\pi^0)K^{*-}$	6.7, 8.0	-0.12 ± 0.07	-0.3 ± 0.2 -0.3 ± 0.2
$B^- \rightarrow D^{*0}(D^0(K^-\pi^+\pi^0)\pi^0)K^{*-}$	2.3, 2.6	3.6 ± 2.0	8.4 ± 4.7 7.5 ± 4.1
$B^- \rightarrow D^{*0}(D^0(K^-\pi^+\pi^+\pi^-)\pi^0)K^{*-}$	3.5, 4.4	0.8 ± 1.5	2.3 ± 4.3 1.8 ± 3.4
$B^- \rightarrow D^{*0}(D^0(K^-\pi^+)\gamma)K^{*-}$	6.0, 6.9	2.9 ± 1.7	15.0 ± 8.8 13.0 ± 7.6
$B^- \rightarrow D^{*0}(D^0(K^-\pi^+\pi^0)\gamma)K^{*-}$	1.9, 2.0	2.7 ± 1.7	12.4 ± 7.8 11.8 ± 7.4
$B^- \rightarrow D^{*0}(D^0(K^-\pi^+\pi^+\pi^-)\gamma)K^{*-}$	3.5, 3.7	6.0 ± 2.7	27.2 ± 12.3 25.7 ± 11.6
$B^- \rightarrow D^{*0}K^{*-}$		$14.6 \pm 4.3 (6.2\sigma)$	8.3 ± 2.4 7.2 ± 2.1

new signal yields, efficiencies and branching ratios. Since the data were collected with two different detector configurations, we have also calculated the branching ratios separately for the two sets of data. If the difference in the branching ratios between the two data sets is larger than the one from varying the selection cuts, this is taken as the systematic error. The variation of cuts contributes the major part of the total systematic error. Systematic errors also include uncertainties from track, shower, K_S^0 and π^0 reconstruction efficiencies and uncertainties from the number of $B\bar{B}$ pairs, the ratio of $B^0\bar{B}^0$ to $B\bar{B}$ in $\Upsilon(4S)$ decays [8] and the $D^{(*)}$ and K^{*-} decay branching fractions [9].

To study the systematic errors from the $\bar{B} \rightarrow D^{(*)}K^{*-}$ fitting procedure, we fit the mass distributions using a background shape obtained from the continuum data for each decay mode. The differences with Table I, which are less than 3%, are taken as the systematic errors of the signal yields. The systematic errors due to uncertainties of the beam-constrained mass resolutions determined from Monte Carlo simulation are less than 3% from studies of similar $\bar{B} \rightarrow D^{(*)}\pi^-$ decays.

The efficiency for observing $\bar{B} \rightarrow D^*K^{*-}$ decays depends on the unknown polarization of the final state. Assuming both final state mesons are in a helicity 0 state, we find $\mathcal{B}(\bar{B}^0 \rightarrow D^{*+}K^{*-}) = (4.1 \pm 1.4 \pm 0.8) \times 10^{-4}$ and $\mathcal{B}(B^- \rightarrow D^{*0}K^{*-}) = (8.3 \pm 2.4 \pm 2.6) \times 10^{-4}$. Should the dynamics of the decay process force the final state mesons into ± 1 helicity states, we find $\mathcal{B}(\bar{B}^0 \rightarrow D^{*+}K^{*-}) = (3.5 \pm 1.2 \pm 0.7) \times 10^{-4}$ and $\mathcal{B}(B^- \rightarrow D^{*0}K^{*-}) = (7.2 \pm 2.1 \pm 2.4) \times 10^{-4}$. The errors are statistical and systematic. Assuming an unpolarized final state, we take the equally-weighted average of the two branching ratios, corresponding

to the 00 and 11 helicity states from Table I, as the central value, and the differences as a systematic error. These differences are small compared to the statistical errors.

We have observed significant signals in the exclusive $\bar{B} \rightarrow D^{(*)}K^{*-}$ decay decays. The measured branching ratios are:

$$\begin{aligned}\mathcal{B}(B^- \rightarrow D^0 K^{*-}) &= (6.1 \pm 1.6 \pm 1.7) \times 10^{-4}, \\ \mathcal{B}(\bar{B}^0 \rightarrow D^+ K^{*-}) &= (3.7 \pm 1.5 \pm 1.0) \times 10^{-4}, \\ \mathcal{B}(\bar{B}^0 \rightarrow D^{*+} K^{*-}) &= (3.8 \pm 1.3 \pm 0.8) \times 10^{-4}, \\ \mathcal{B}(B^- \rightarrow D^{*0} K^{*-}) &= (7.7 \pm 2.2 \pm 2.6) \times 10^{-4}.\end{aligned}$$

The errors shown are statistical and systematic, respectively.

With the assumption of the validity of factorization, $SU(3)$ flavor symmetry relates the Cabibbo-suppressed decays $\bar{B} \rightarrow D^{(*)}K^{*-}$ to the Cabibbo-favored ones $\bar{B} \rightarrow D^{(*)}\rho^-$ by $\frac{\mathcal{B}(\bar{B} \rightarrow D^{(*)}K^{*-})}{\mathcal{B}(\bar{B} \rightarrow D^{(*)}\rho^-)} \simeq \left| \frac{V_{us}}{V_{ud}} \right|^2 \left(\frac{f_{K^{*-}}}{f_{\rho^-}} \right)^2 \simeq 5\%$ in the tree level approximation. Here, V_{us} and V_{ud} are CKM elements, and $f_{K^{*-}}$ and f_{ρ^-} are the meson decay constants which can be derived from $\tau^- \rightarrow K^{*-}\nu_\tau$ and $\tau^- \rightarrow \rho^-\nu_\tau$ decays. For the above decay modes, the measured ratios $\frac{\mathcal{B}(\bar{B} \rightarrow D^{(*)}K^{*-})}{\mathcal{B}(\bar{B} \rightarrow D^{(*)}\rho^-)}$ are $(4.6 \pm 1.8)\%$, $(4.7 \pm 2.4)\%$, $(5.6 \pm 3.6)\%$ and $(5.0 \pm 2.4)\%$ respectively, which are consistent with naive theoretical predictions within the errors [14]. The branching ratios for $\bar{B} \rightarrow D^{(*)}\rho^-$ decays are taken from PDG 2000 [9]. The rates for $\bar{B} \rightarrow D^{(*)}K^{*-}$ suggest that these decays could provide a measurement of the angle γ in the unitary triangle using the color-allowed decays in the near future [15].

ACKNOWLEDGMENTS

We gratefully acknowledge the effort of the CESR staff in providing us with excellent luminosity and running conditions. This work was supported by the National Science Foundation, the U.S. Department of Energy, the Research Corporation, and the Texas Advanced Research Program.

REFERENCES

- [1] M. Kobayashi and T. Maskawa, Prog. Theor. Phys. **49**, 652 (1973).
- [2] P. F. Harrison and H. R. Quinn, The BaBar Physics Book (SLAC-R-0504, 1998).
- [3] M. Gronau and D. Wyler, Phys. Lett. **B265**, 172 (1991); I. Dunietz, Phys. Lett. **B270**, 75 (1991); D. Atwood, G. Eilam, M. Gronau and A. Soni, Phys. Lett. **B341**, 372 (1995); D. Atwood, I. Dunietz and A. Soni, Phys. Rev. Lett. **78**, 3257 (1997).
- [4] CLEO Collaboration, M. Athanas *et al.*, Phys. Rev. Lett. **80**, 5493 (1998).
- [5] BELLE Collaboration, K. Abe *et al.*, Phys. Rev. Lett. **87**, 111801 (2001).
- [6] CLEO Collaboration, Y. Kubota *et al.*, Nucl. Instrum. Methods A **320**, 66 (1992).
- [7] T. Hill, Nucl. Instrum. Methods A **418**, 32 (1998).
- [8] CLEO Collaboration, J. Alexander *et al.*, Phys. Rev. Lett. **86**, 2737 (2000).
- [9] Particle Data Group, D. E. Groom *et al.*, Eur. Phys. J. **C15**, 1-878 (2000).
- [10] CLEO Collaboration, S. Kopp *et al.*, Phys. Rev. D **63**, 092001 (2001).
- [11] S. L. Wu, Phys. Rep. C **107**, 59 (1984).
- [12] ARGUS Collaboration, H. Albrecht *et al.*, Z. Phys. C **48**, 543 (1990).
- [13] R. Burn *et al.*, GEANT3.14, CERN DD/EE/84-1 (unpublished).
- [14] Similar ratios are $\frac{\mathcal{B}(\bar{B} \rightarrow D^{(*)} K^-)}{\mathcal{B}(B \rightarrow D^{(*)} \pi^-)} \simeq \left| \frac{V_{us}}{V_{ud}} \right|^2 \left(\frac{f_K}{f_\pi} \right)^2 \simeq 7\%$. The results of $\frac{\mathcal{B}(\bar{B} \rightarrow D^{(*)} K^-)}{\mathcal{B}(B \rightarrow D^{(*)} \pi^-)}$ from BELLE are consistent with the naive model calculation, see Ref. [5].
- [15] M. Gronau, Phys. Rev. D **58**, 037301 (1998); J. H. Jang and P. Ko, Phys. Rev. D **58**, 111302 (1998).